2004-01-1366

Cylinder Air Charge Estimator in Turbocharged SI-Engines

Per Andersson, Lars Eriksson

Vehicular Systems, ISY
Linköping University
SE-581 83 Linköping, SWEDEN
Email: {peran,larer}@isy.liu.se

ABSTRACT

Mean value cylinder air charge (CAC) estimation models for control and diagnosis are investigated on turbocharged SI-engines. Two topics are studied; Firstly CAC changes due to fuel enrichment and secondly CAC sensitivity to exhaust manifold pressure changes. The objective is to find a CAC model suitable for control and diagnosis.

Measurements show that CAC models based on volumetric efficiency gives up to 10% error during fuel enrichment. The error is caused by the cooling effect that the fuel has as it evaporates and thus increases the charge density. To better describe the CAC during fuel enrichment a simple one parameter model is proposed which reduces the CAC estimation error on experimental data from 10% to 3%.

With active wastegate control, the pressure changes in the exhaust manifold influences the CAC. The magnitude of this influence is investigated using sensitivity analysis on an exhaust manifold pressure dependent CAC-model. From the sensitivity analysis it can be concluded, that the CAC is most sensitive to exhaust manifold pressure changes for low intake manifold pressures (part load). Without taking the exhaust manifold pressure into account the CAC error is approximately 5% when the wastegate is opened at part load.

The exhaust manifold pressure dependent CAC model is then augmented with the charge cooling model and the total model gives precise agreement on experimental data. The resulting model is thus highly suitable for CAC estimation for control and diagnosis of turbocharged SI-engines.

INTRODUCTION

Turbocharged SI-engines is a concept for the future since it enables both good fuel economy and low emissions [1]. Further improvements and research on such engines are therefore highly important. Here cylinder air charge (CAC) models based on speed-density principles are studied for control and diagnosis.

Emissions from SI-engines can be kept very low using a three way catalyst, provided that the air-fuel ratio control is accurate [2, 3, 4]. A key element in precise air/fuel control is the CAC estimation [5, 6, 7]. Good CAC estimates can also be beneficial for torque estimation [4, pp. 57], and can be used for diagnosis [8] of the intake system [9].

Here special attention is given to two topics in CAC. First the influence of fuel enrichment at high loads is studied. At rich conditions standard CAC models predicts a decrease in estimated CAC and the magnitude of the error is up to 10%. To improve the CAC estimates at rich conditions a one parameter model is introduced that describes the charge cooling effect of the evaporating fuel. The augmented model can for example be used to provide better torque estimates or to prevent false alarms in diagnosis systems for sensors etc.

The second topic is how the CAC estimate is influenced by exhaust manifold pressure changes caused by openings and closings of the wastegate. It is desirable to open the wastegate at part load to reduce the pumping losses and therefore improve the fuel economy [10]. A side effect of opening and closing the wastegate is that the changing exhaust manifold pressure influences the CAC with a non-negligible 5%. The objective of the study is to answer the question whether it is necessary to include exhaust manifold pressure in the CAC model when active wastegate control is used.

The two studied topics are validated using experimental tests performed on a 2.3 liter turbocharged SAAB 9^5 engine with wastegate (B235R).

CAC AND AIR/FUEL RATIO

Normally the engine runs with stoichiometric air/fuel ratio but at full power engines can use fuel enrichment. This enrichment also has the side effect of influencing the CAC, which will be thoroughly studied and an augmented model

is suggested. Here CAC is defined as the mass of air trapped in the cylinder per cycle.

Volumetric efficiency [4, p. 53] is a parameter that describes how well the cylinder is filled with air. Using the volumetric efficiency the CAC can be estimated as:

$$\mathrm{CAC} = \eta_{\mathrm{vol}} \frac{p_{\mathrm{im}} V_{\mathrm{d}}}{R_{\mathrm{im}} T_{\mathrm{im}}} \tag{1}$$

For stationary conditions the volumetric efficiency can be determined using measured air-mass flow W_{a} as

$$\eta_{\mathrm{vol_{meas}}} = \frac{W_{\mathrm{a}} R_{\mathrm{im}} T_{\mathrm{im}} n_{\mathrm{r}}}{p_{\mathrm{im}} V_{\mathrm{d}} N} \tag{2}$$

This equation does not include the air/fuel ratio and will be used to represent measured volumetric efficiency when it is compared to the theoretical behavior. If only the fuel vapor volume is considered the volumetric efficiency theoretically depends on the air/fuel ratio as [4, p. 210]:

$$\eta_{\mathrm{vol_{theor}}} \propto \frac{1}{1 + \frac{1}{\left(\frac{A}{F}\right)_s \lambda}} \tag{3}$$

Equation (3) describes that the volume of air is inversely proportional to the volume of fuel vapor, which means the volumetric efficiency should decrease as the air/fuel ratio decreases. In the bottom of Figure 1 this decrease is illustrated. For measured volumetric efficiency, shown in the top of Figure 1, the opposite phenomenon occurs. This behavior can not be explained by other volumetric efficiency increasing effects such as intake manifold tuning or RAM-effect.

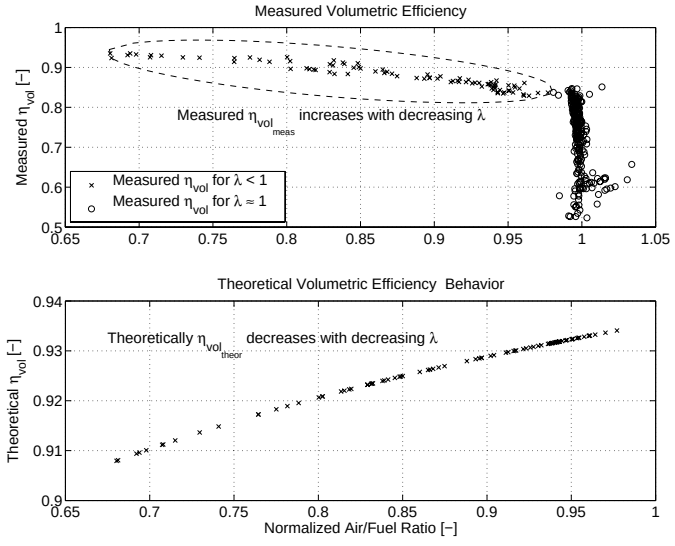

Figure 1: *Top:* The estimated volumetric efficiency η_{vol} from measurements with various air/fuel ratios λ. For low λ the volumetric efficiency η_{vol} increases significantly. *Bottom:* Theoretically the volumetric efficiency should decrease with decreasing λ as the fraction of fuel vapor increases.

One explanation is the charge cooling effect the additional fuel has when it evaporates and uses energy from the surroundings in the evaporation process. Thus the density increases more than the increased fuel vapor volume decreases the volumetric efficiency [4, pp. 211]. In [11, pp. 184] a similar explanation is given. This knowledge can be included in the CAC-estimation using a model of the charge cooling as the fuel evaporates.

MODELING OF CHARGE COOLING BY FUEL EVAPORATION

In Figure 2 a schematic of the intake system is shown. When the gas have entered the intake manifold it is heated by $\dot{Q}_{\mathrm{man}}$ to the measured temperature T_{im}. During the induction phase the gas entering the cylinder is cooled by the evaporating fuel and heated by the hot intake valve and the cylinder $\dot{Q}_{\mathrm{valve\ and\ cylinder}}$ to the final in cylinder temperature T_{cyl}.

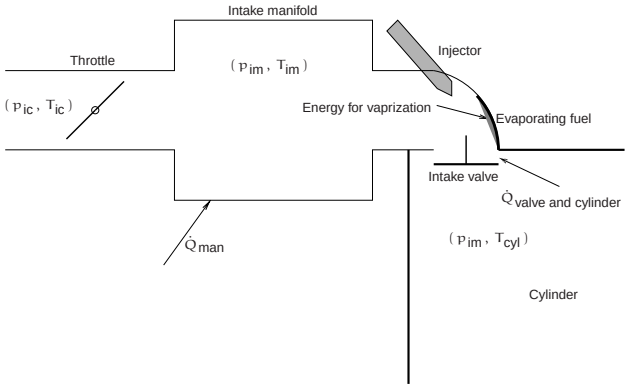

Figure 2: A schematic of the intake manifold with throttle and injector. Where there is heat transfer, the direction of the heat transfer is indicated by the arrows. The air enters the intake manifold with temperature T_{ic} and is heated to the measured temperature T_{im} by $\dot{Q}_{\mathrm{man}}$. The injector is located close to the intake valve and it injects the fuel on the valve and on the walls. When the fuel evaporates it uses energy from the air. Finally heat is added when the charge is inducted to the cylinder $\dot{Q}_{\mathrm{valve\ and\ cylinder}}$.

The temperature change during the induction, caused by the heating $\dot{Q}_{\mathrm{valve\ and\ cylinder}}$ and cooling by fuel vaporization [4, pp. 211], is estimated using the following equation:

$$T_{\mathrm{cyl}} - T_{\mathrm{im}} = \frac{\dot{Q}_{\mathrm{valve\ and\ cylinder}}/W_{\mathrm{a}} - \overbrace{x_e (F/A) h_{\mathrm{f,LV}}}^{\text{Vaporization energy}}}{c_{\mathrm{p,a}} + (F/A) c_{\mathrm{f,L}}}$$

W_{a} is the air-mass flow, x_e is the fraction of evaporated fuel which is assumed to be constant, $(F/A) = \frac{1}{\left(\frac{A}{F}\right)_s \lambda}$ is the fuel air ratio, $h_{\mathrm{f,LV}}$ is the enthalpy of vaporization of the fuel, $c_{\mathrm{p,a}}$ is the specific heat of air, and finally $c_{\mathrm{f,L}}$ is the heat capacity of liquid fuel. As the last term in the denominator is small, for normal gasoline, the equation

simplifies to

$$T_{cyl} - T_{im} \approx \frac{\dot{Q}_{\text{valve and cylinder}}/W_a - x_e \frac{1}{\left(\frac{A}{F}\right)_s \lambda} h_{f,LV}}{c_{p,a}}$$

As the volumetric efficiency gives a good description of the CAC during stoichiometric conditions, the focus is moved to non-stoichiometric conditions. Therefore only the *additional* cooling compared to stoichiometric conditions is modeled. That is $(T_{cyl}(\lambda) - T_{im}) - (T_{cyl}(\lambda = 1) - T_{im})$ which is described by:

$$\underbrace{T_{cyl}(\lambda) - T_{cyl}(\lambda = 1)}_{\text{Additional charge cooling}} = \underbrace{x_e \frac{h_{f,LV}}{c_{p,a}} \frac{1}{\left(\frac{A}{F}\right)_s}}_{\text{constant}=C_1} \left(\frac{1}{\lambda} - 1\right) \quad (4)$$

Now, when a model of the additional charge cooling exists it can be included in the CAC-estimation, where it is included as a temperature drop in intake manifold temperature.

CAC MODEL WITH CHARGE COOLING

A model that describes CAC at stoichiometric conditions well will be augmented with the charge cooling model that describes the cooling effect of additional fuel.

In [12] it is shown that it is possible to parameterize the product $\eta_{vol} p_{im}$ in Equation (1) as an affine function in p_{im}, which describes the CAC for stoichiometric conditions with a high accuracy:

$$CAC = (a_1 p_{im} + a_0) \frac{V_d}{R_{im} T_{im}} \quad (5)$$

To include the effect of the additional charge cooling by fuel evaporation the a temperature drop described by Equation (4) is subtracted from the measured T_{im} and the temperature T_{im} in Equation (5) is replaced with

$$T_{im,new} = T_{im} - C_1 \left(\frac{1}{\lambda} - 1\right) \quad (6)$$

By inserting Equation (6) in Equation (5) the following CAC-model is available:

$$CAC = (a_1 p_{im} + a_0) \frac{V_d}{R_{im}\left(T_{im} - \underbrace{C_1 \left(\frac{1}{\lambda} - 1\right)}_{\text{Charge cooling}}\right)} \quad (7)$$

In Equation (7) the parameter C_1 is identified together with a_1 and a_0 using a nonlinear least-squares technique for stationary data.

RESULTS USING THE CHARGE COOLING MODEL

A comparison between measured and estimated CAC using Equation (7) with and without the proposed cooling model Equation (6) is shown in Figure 3. The model that includes the charge cooling effect reduces the stationary error at high CAC from 10% down to 2–3%.

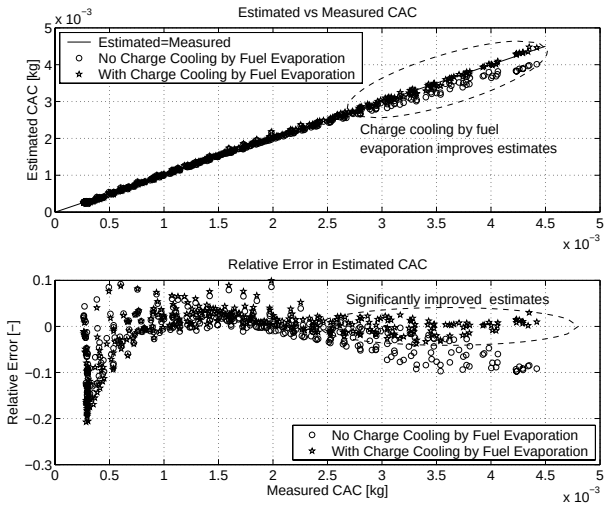

Figure 3: *Top:* Measured CAC for stationary engine data is compared to estimated CAC with charge cooling, Equation (7), and estimated CAC without charge cooling, Equation (5). When enrichment is present, the model without charge cooling by fuel evaporation gives up to 10% too low estimates. *Bottom:* With the modeled effect of charge cooling by fuel evaporation the error in CAC is substantially reduced down to 2–3% for higher CACs.

In Figure 4 the model is applied to measured engine data and the estimated additional temperature drop is less than approximately 15%. For iso-octane the temperature drop is approximately 2% and for methanol the maximum drop would be around 30% [4, p. 211]. The estimated temperature drop for rich mixtures is in between these values which increases the credibility of the model. A contributing factor to the result is that winter gasoline is used. Winter gasoline vaporizes at a lower temperature, has a higher volatility [13, p. 233], and can have a higher content of alcohols. Also the assumption of constant x_e is motivated in Figure 3 as modeled CAC shows a very good agreement with measured CAC over a wide range of operating points.

With this approach the main advantages are:

- The temperature drop for rich mixtures caused by charge cooling can be treated using an augmentation of the intake manifold temperature model.
- The model has only one parameter C_1 which is easily tuned.

CAC AND EXHAUST PRESSURE CHANGES

It has been shown in [10] that the fuel economy can be improved if the wastegate is opened at part load. The fuel economy is improved as the opening of the wastegate reduces the pumping losses and therefore increases the engine efficiency. At part load the engine is running

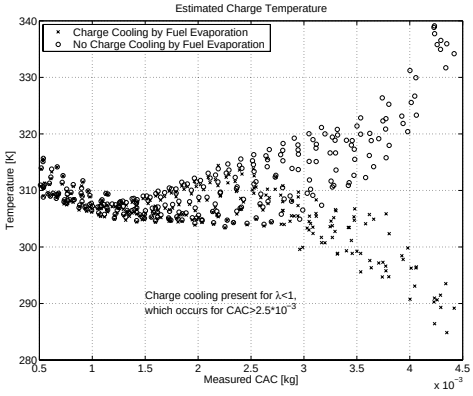

Figure 4: Results when applying the charge cooling by fuel evaporation model to get the mixture temperature for stationary measured data. The modeled temperature drop is approximately 15% for the highest CAC.

stoichiometricly and with active wastegate control it is important to make precise estimates of the CAC to maintain the stoichiometric mixture. The necessary accuracy of the CAC estimate is approximately 2% to 3% [14, pp. 69].

In Figure 5 an experiment is shown on the engine in the research laboratory where the wastegate is opened and closed at constant engine speed. From Figure 5 it is clear that CAC estimates made using the mapped volumetric efficiency is incorrect for open wastegate due to the stationary difference between measured and mapped volumetric efficiency. The stationary volumetric efficiency difference is caused by the exhaust manifold pressure change when the wastegate is opened [15]. The reduced exhaust manifold pressure reduces the amount of residual gases in the cylinder and thus increases the volumetric efficiency. This raises following questions:

1. Under which operating conditions is the CAC most sensitive to exhaust manifold pressure changes?

2. Given a desired accuracy of the estimated CAC: How large exhaust manifold pressure changes can be allowed with an exhaust manifold pressure independent model?

To answer the questions a CAC sensitivity analysis is performed. It is performed using an ideal model of CAC [10] that includes exhaust manifold pressure. This model is first validated, for stationary data, and compared to a standard volumetric efficiency based CAC model Equation (5). In the comparison the high accuracy of the exhaust manifold pressure dependent model is shown before the sensitivity analysis is performed.

CAC MODEL WITH EXHAUST MANIFOLD PRESSURE DEPENDENCY

The purpose of the model is CAC estimation for primarily air/fuel ratio-control with the possibility to take exhaust manifold pressure into account.

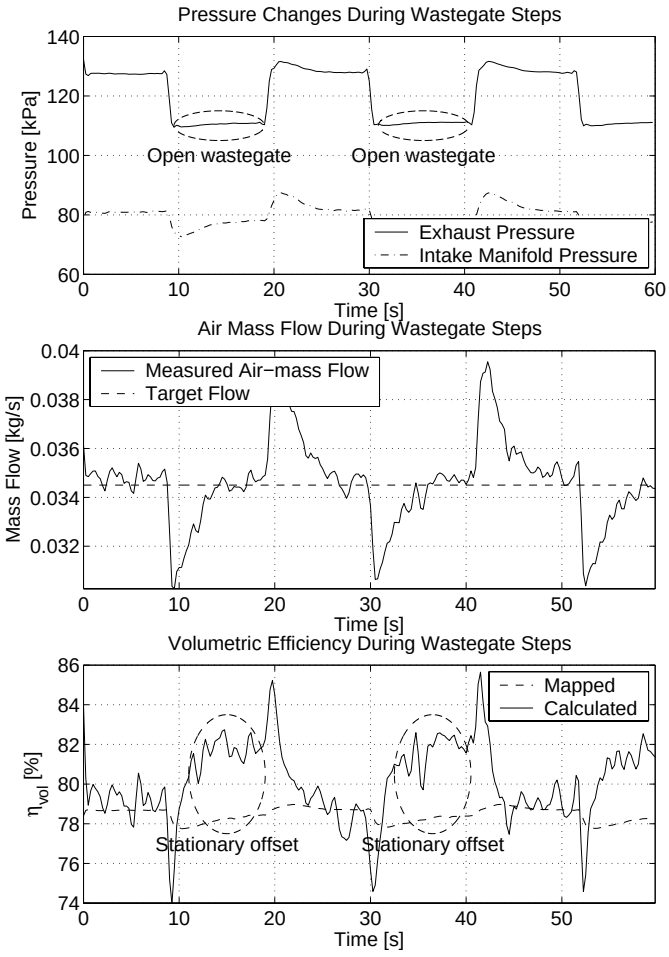

Figure 5: An engine experiment performed at constant speed and constant air-mass flow. *Top:* Pressure changes in exhaust system, and intake manifold pressure during manual opening/closing of the wastegate. *Center:* Measured air-mass flow, W_a. As the wastegate is opened the air-mass flow decreases momentarily while the air-mass controller opens the throttle. *Bottom:* Mapped and calculated volumetric efficiency using Equation (2). The calculated volumetric efficiency is only valid at stationary conditions which are marked with ellipsises. When the wastegate is open the mapped volumetric efficiency is incorrect. The change is $(82-78)/78 \approx$5% which would result in a 5% CAC error.

In Figure 6 it is illustrated how the volume of air V_a and evaporated fuel V_f can simply be estimated by subtracting the residual gas volume at intake valve closing (IVC) from the total volume. A more detailed derivation of the model below is found in Appendix A:

$$\mathrm{CAC} = \frac{\overbrace{p_{im}\, C_{\eta_{vol}} \frac{1}{1+\frac{1}{\lambda\left(\frac{A}{F}\right)_s}} \left(\frac{r_c - \left(\frac{p_{em}}{p_{im}}\right)^{\frac{1}{\gamma_e}}}{r_c - 1} \right) V_d}^{V_a}}{R_{im} T_{im}} \qquad (8)$$

The effect of charge cooling by fuel evaporation can also be included in Equation (8) by replacing T_{im} with Equa-

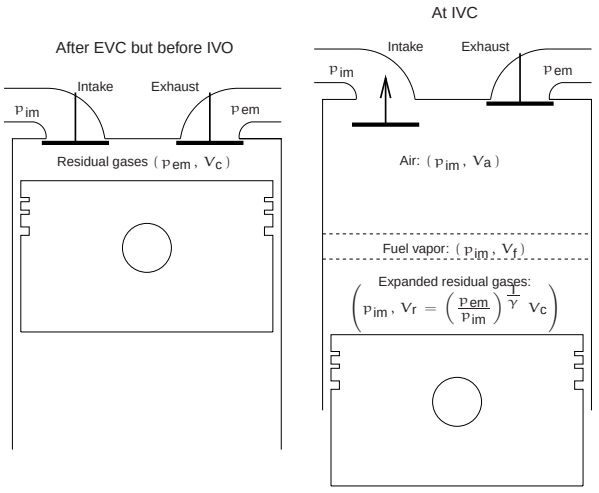

Figure 6: An illustration of the idealized induction model. *Left:* Before the inductions starts, at exhaust valve closing (EVC), the volume of residual gases is V_c and the pressure is the same as in the exhaust manifold p_{em}. *Right:* At the end of the intake stroke, when the intake valve is about to close, the total volume is $V_d + V_c$. In all of the volumes at IVC the pressure is assumed to be the same (p_{im}). Each volume is shown separated by a dashed line.

tion (6) which has been done in Equation (9).

$$\mathrm{CAC} = p_{im} C_{\eta_{vol}} \frac{1}{1 + \frac{1}{\lambda \left(\frac{A}{F}\right)_s}} \frac{r_c - \left(\frac{p_{em}}{p_{im}}\right)^{\frac{1}{\gamma_e}}}{r_c - 1} V_d \cdot \frac{1}{R_{im}\left(T_{im} - \underbrace{C_1\left(\frac{1}{\lambda} - 1\right)}_{\text{Charge cooling}}\right)} \quad (9)$$

In Equation (9) a CAC model has been introduced with dependencies on exhaust manifold pressure and charge cooling by fuel evaporation. The model has only two semi-physical tuning parameters and these are the pumping parameter $C_{\eta_{vol}}$ and the effect of charge cooling by fuel evaporation C_1.

Model Validation Using Stationary Data

A validation is performed using stationary data. The exhaust manifold pressure dependent model and a model based on a parameterization of the volumetric efficiency are compared to measured CAC. The purpose of this comparison is to show:

1. The high accuracy of the exhaust manifold pressure dependent model given by Equation (9) on validation data.
2. That the model using exhaust manifold pressure has the same accuracy, for a nominal wastegate setting, as models based on volumetric efficiency such as Equation (5).

In this validation two separate datasets are used, one to build the models and another to validate the models. In both cases the wastegate is controlled to a nominal opening by the ECU, which means that it is closed for most of the points.

The high accuracy of the exhaust manifold pressure dependent model is shown in the top of Figure 7 where it is compared to the model using parameterized volumetric efficiency. Both models give the same accuracy for medium to large CAC where in this case also fuel enrichment is present. The exhaust manifold pressure dependent model shows slightly better behavior for low CAC and it is important to note that it gives this accuracy even though it has one parameter less.

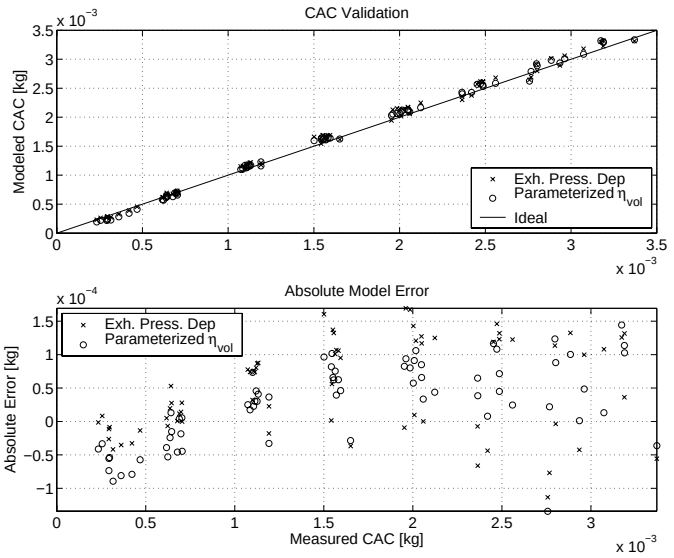

Figure 7: Validation of the exhaust manifold pressure dependent CAC model using stationary data. It is compared to a model using parameterized volumetric efficiency and measured data. The accuracy of Equation (9) is in the same magnitude as the model using parameterized volumetric efficiency, Equation (7), except for very low CAC where it shows a slightly better precision.

Model Validation Using Changing Pressure

In Figure 8 the wastegate is opened and closed several times and the exhaust manifold pressure dependent model, Equation (9), is better at stationary condition in predicting the CAC *change* than the parameterized volumetric efficiency, Equation (7). It has not been possible to measure the transient CAC and therefore the estimates are compared to measured air-mass flow after the air filter. This means that the comparison in Figure 8 is only valid for stationary conditions due to the filling and emptying of the intake system. The locations of the stationary conditions when the wastegate is open have been marked using ellipsis. Both models have been tuned for nominal wastegate settings, which in this case is closed wastegate. The model in Equation (9) is able to better estimate

the change in CAC when the wastegate is open which is a condition where the model has not been tuned. This property makes it suitable for studies of CAC sensitivity to exhaust manifold pressure changes.

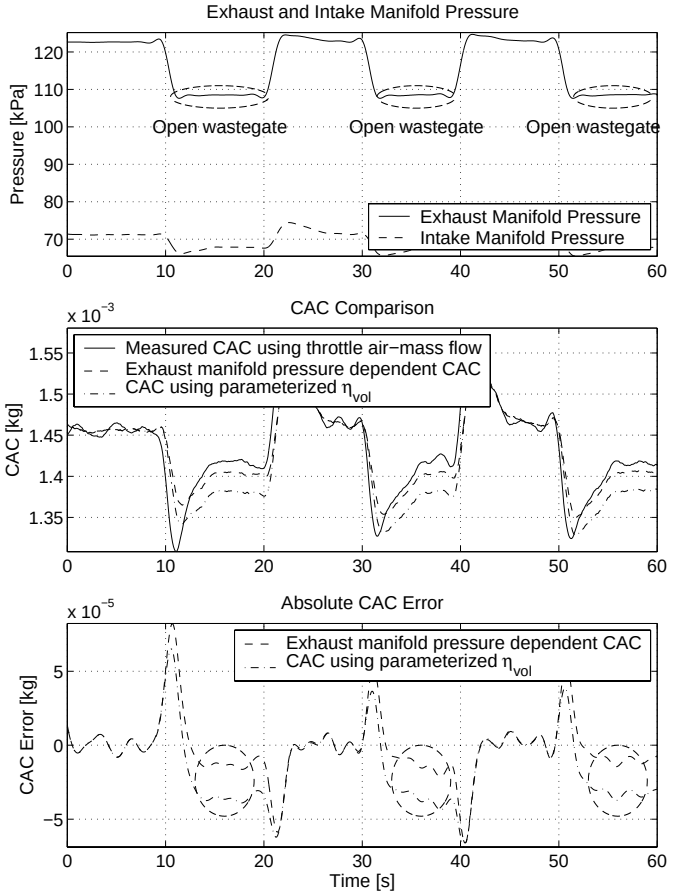

Figure 8: Validation using wastegate opening/closing steps. *Top:* Intake manifold pressure and exhaust manifold pressure when the wastegate is opened or closed. *Center:* The estimated CAC compared to measured CAC. Note that stationary errors for closed wastegate have been removed for both models in order to study the estimated change in CAC when the wastegate opens. The CAC based on parameterized volumetric efficiency underestimates CAC when the wastegate is open. *Bottom:* The absolute error for the model using parameterized volumetric efficiency is larger when the wastegate is open compared to the exhaust manifold pressure dependent model.

CAC SENSITIVITY FUNCTIONS

Now an accurate CAC model exists that takes exhaust manifold pressure into account. This model can therefore be used to study the CAC sensitivity to changes in exhaust manifold pressure using sensitivity functions. The CAC sensitivity to the parameter x is defined as:

$$\frac{\frac{\partial CAC}{\partial x}}{\frac{CAC}{x}}$$

CAC Sensitivity to Exhaust Manifold Pressure Changes

The derivative of Equation (9) with respect to the exhaust manifold pressure is determined and then divided by Equation (9) and p_{em} which yields the sensitivity to exhaust manifold pressure changes:

$$\frac{\frac{\partial CAC}{\partial p_{em}}}{\frac{CAC}{p_{em}}} = -\left(\frac{p_{em}}{p_{im}}\right)^{\frac{1}{\gamma_e}} \frac{1}{\gamma_e\left(r_c - \left(\frac{p_{em}}{p_{im}}\right)^{\frac{1}{\gamma_e}}\right)} \qquad (10)$$

The minus sign in Equation (10) means that an increased exhaust manifold pressure decreases CAC. In Figure 9 the sensitivity function is shown for some fix intake manifold pressures. From the figure it is clear that the CAC is most sensitive to changes in p_{em} for low intake manifold pressures. This is important since at part load conditions, where it is most desirable to open the wastegate, corresponds to low intake manifold pressures.

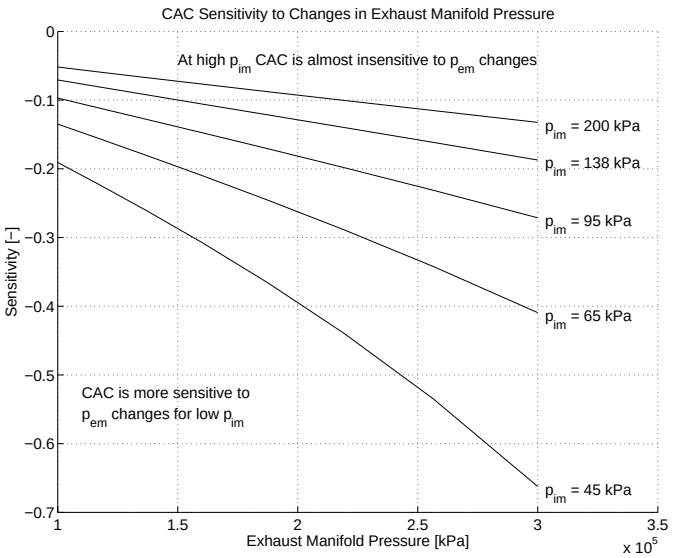

Figure 9: Sensitivity to exhaust manifold pressure changes is negative. It means that for a given intake manifold pressure CAC therefore decreases with increasing exhaust manifold pressure. For high intake manifold pressures CAC is almost insensitive to p_{em}-changes.

CAC Sensitivity to Intake Manifold Pressure Changes

The derivative of Equation (9) with respect to the intake manifold pressure is determined and then divided by Equation (9) and p_{im} which yields the sensitivity to intake manifold pressure changes:

$$\frac{\frac{\partial CAC}{\partial p_{im}}}{\frac{CAC}{p_{im}}} = 1 + \frac{\left(\frac{p_{em}}{p_{im}}\right)^{\frac{1}{\gamma_e}}}{\gamma_e\left(r_c - \left(\frac{p_{em}}{p_{im}}\right)^{\frac{1}{\gamma_e}}\right)} \qquad (11)$$

In Figure 10 the sensitivity function is shown for various intake manifold pressures. If the wastegate is used at part

load the sensitivity is approximately 5 times larger than the sensitivity to exhaust manifold pressure changes.

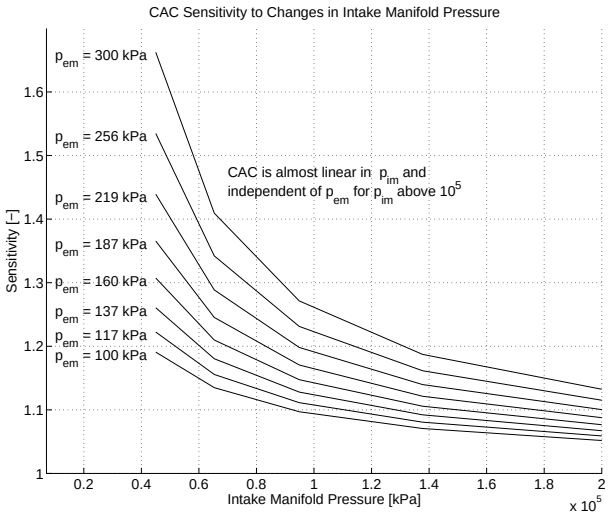

Figure 10: CAC is most sensitive to intake manifold pressure changes for low intake manifold pressures.

Sensitivity Function Usage

One advantage of the sensitivity functions, Equations (10) and (11), is that they do not include any specific engine parameters which require tuning to measured data. This makes the results from the sensitivity functions very general.

An example is given to describe how the sensitivity functions are used. In the example the change in CAC is estimated at $p_{im} = 60$ kPa for an exhaust manifold pressure drop of $\Delta p_{em} = 30$ kPa from an initial $p_{em} = 145$ kPa:

$$\underbrace{-0.21}_{\frac{\frac{\partial CAC}{\partial p_{em}}}{\frac{CAC}{p_{em}}}} \cdot \underbrace{\frac{-30 \cdot 10^3}{145 \cdot 10^3}}_{\text{Pressure drop fraction}} \approx 0.0428$$

That is CAC increases by 4%. In this example a small error has been made in that the sensitivity is not constant along the exhaust manifold pressure change, see for example the 65 kPa line in Figure 9. If the sensitivity in the example is evaluated using the step in the other direction that is from $p_{em} = 115$ kPa and $\Delta p_{em} = 30$ kPa the result is a decrease in CAC with:

$$\underbrace{-0.17}_{\frac{\frac{\partial CAC}{\partial p_{em}}}{\frac{CAC}{p_{em}}}} \cdot \underbrace{\frac{30 \cdot 10^3}{115 \cdot 10^3}}_{\text{Pressure drop fraction}} \approx -0.0433$$

The difference in sensitivity is negligible compared to the step in the first direction, which means that for pressure changes caused by openings/closings of the wastegate the result is independent of the step direction.

From this example it is clear that it is necessary to know the magnitude of the exhaust manifold pressure drop when the wastegate is opened/closed.

EXHAUST MANIFOLD PRESSURE DROP

The maximum achievable pressure change when the wastegate goes from closed to open position can be determined by measuring the exhaust manifold pressure on the running engine with the wastegate fully opened and closed. In Figure 7 the exhaust manifold pressure drop is shown for various air-mass flows. The maximum possible pressure drop is slightly more than 20%.

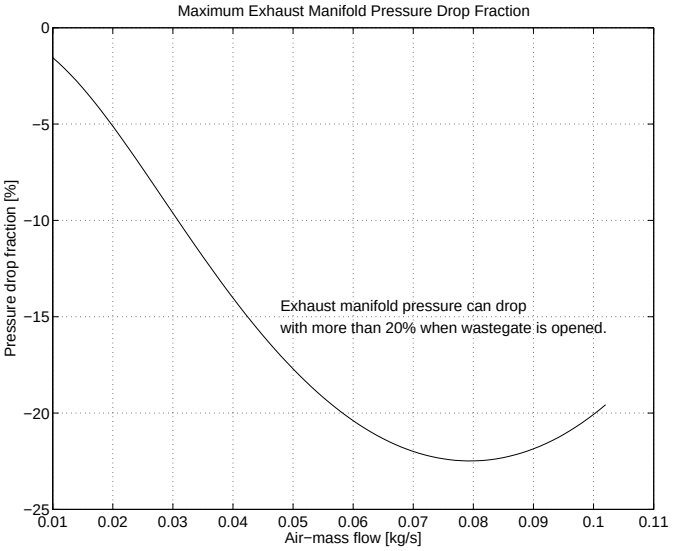

Figure 11: The exhaust manifold pressure drop that can be achieved by opening the wastegate. On this engine the exhaust manifold pressure can be reduced with more than 20% by opening the wastegate.

CAC SENSITIVITY TO EXHAUST MANIFOLD PRESSURE CHANGES

The result from Figure 11 is used to determine how sensitive the CAC is to changes in exhaust manifold pressure caused by wastegate openings and closings. When the wastegate is open the power to the turbine drops and there is no boost pressure. The maximum intake manifold pressure is therefore limited to 1 atm (ambient pressure).

By applying the sensitivity function Equation (10) on a measured engine map for intake manifold pressures lower than ambient pressure to the maximum possible exhaust manifold pressure drop, from Figure 11, the resulting maximum deviation in CAC is 5%. The estimated change in CAC when the wastegate goes from fully closed to fully open is shown in Figure 12. The maximum change in CAC is 5%, which corresponds very well to the measured results in Figure 5.

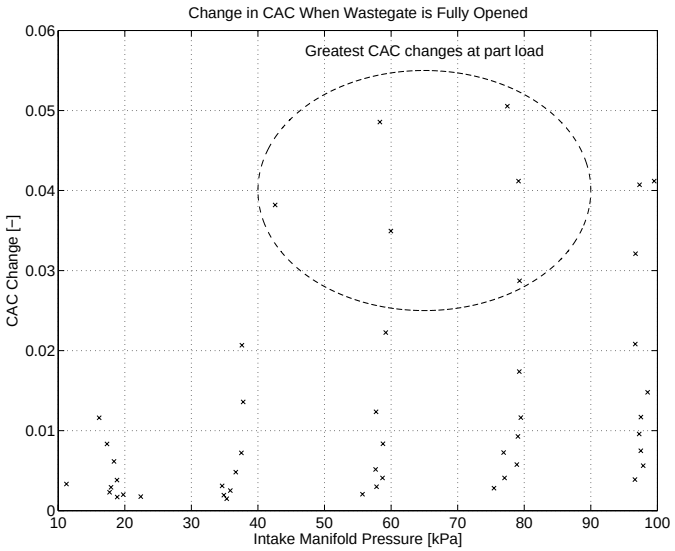

Figure 12: Estimated CAC change when the wastegate goes from fully closed to fully open for mapped engine data. By applying the pressure drop fraction from Figure 11 the change in CAC is estimated using Equation (10) is estimated. At part load there can be an up to 5% increase in CAC.

SUITABLE CAC MODEL FOR CONTROL AND DIAGNOSIS

As standard CAC models for control based on volumetric efficiency do not include exhaust manifold pressure, it is interesting to determine how large exhaust manifold pressure fraction drop $\frac{\Delta p_{em}}{p_{em}}$ that can be allowed before the CAC error is larger than a desired limit. The base for this investigation is that the necessary accuracy of air/fuel ratio controllers is 2% to 3% [14, pp. 69] during stoichiometric conditions. Here the higher CAC error of 3% is used to determine the maximum allowable exhaust manifold pressure drop.

Now, assuming that the exhaust manifold pressure dependent model, Equation (9), gives correct estimates of CAC. The relative error, x in CAC, can be calculated for the model based on parameterized volumetric efficiency as:

$$\frac{\overbrace{\mathrm{CAC}(p_{im})}^{\text{Equation (7)}} - \overbrace{\mathrm{CAC}(p_{im}, p_{em} + \Delta p_{em})}^{\text{Equation (9)}}}{\mathrm{CAC}(p_{im}, p_{em} + \Delta p_{em})} = x \qquad (12)$$

Using $x = 0.03$ in Equation (12) and then solve for Δp_{em} at a given operating point in p_{im} and p_{em} from a measured engine map.

In Figure 13 the required pressure drop for a 3% error in CAC is shown as crosses and the maximum possible exhaust manifold pressure drop fraction when the wastegate goes from closed to fully open from Figure 11 is shown as a line. Crosses above the line indicates that a CAC estimation method independent of exhaust manifold pressure gives an error larger than 3%. This means that if active wastegate control is to be used the CAC estimation must use an exhaust manifold pressure dependent model like Equation (9) to maintain stoichiometric conditions.

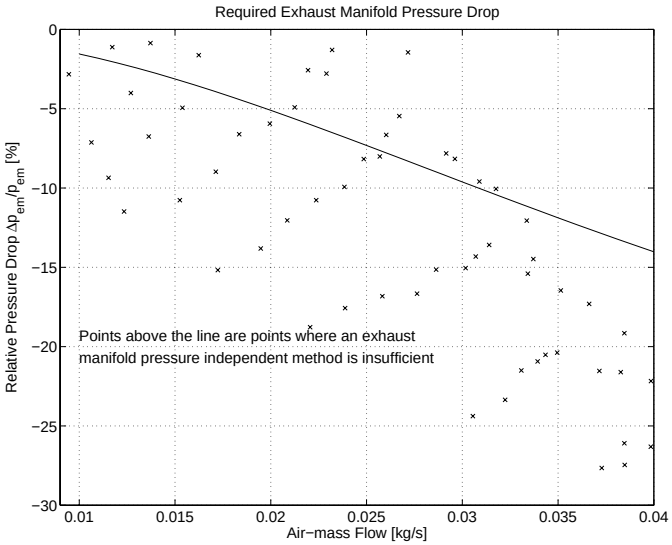

Figure 13: The crosses mark how large exhaust manifold pressure drop in percent that can be accepted before an exhaust manifold pressure independent method gives a CAC error larger than 3%.

RESULTS OF CAC EXHAUST MANIFOLD PRESSURE DEPENDENCY ANALYSIS

Using sensitivity analysis on an exhaust manifold pressure dependent CAC model it has been investigated how the exhaust manifold pressure influences CAC. From the sensitivity analysis there are mainly three results:

- At part load CAC is approximately five time more sensitive to changes in intake manifold pressure than to exhaust manifold pressure changes.
- Sensitivity to changes in exhaust manifold pressure is most significant at part load conditions.
- With active wastegate control at part load the moderate pressure drop when the wastegate is opened results in CAC changes that is not properly described by an exhaust manifold pressure independent CAC model.

One benefit of the analysis is that it does not include any parameters that have to be tuned for a specific engine which makes the results general.

SUMMARY AND CONCLUSIONS

Cylinder air charge (CAC) models have been studied for turbocharged SI-engines. The objective has been to investigate whether standard mean value models based on volumetric efficiency can be used or how improvements can be made to find a good model for control and diagnosis. Two topics have been studied:

1. CAC during fuel enrichment.
2. Exhaust manifold pressure influence on CAC.

At high loads where rich air/fuel ratios are used, the additional fuel influences CAC and standard models give an error of up to 10%. The error is caused by the charge cooling effect that the fuel has when it evaporates and thus increases the charge density. The charge cooling effect is modeled and introduces only one additional parameter. A standard CAC model is then augmented with the charge cooling model. With the augmented CAC model the estimation error at rich conditions is reduced from 10% down to 3%.

CAC depends on the exhaust manifold pressure. This exhaust manifold pressure dependency is not described by standard volumetric efficiency based CAC models. A CAC model that includes exhaust manifold pressure is therefore examined. The model shows good agreement with measured data even for operating conditions where it has not been tuned. Furthermore a sensitivity analysis is performed of the CAC and it can be concluded that:

- Exhaust manifold pressure influences CAC at most for part load conditions.
- It is necessary to include exhaust manifold pressure as CAC models independent of exhaust manifold pressure gives errors larger than 3% when the wastegate is opened.

When the exhaust manifold pressure dependent CAC model is augmented with the charge cooling model, the total model is able to describe CAC with changing exhaust manifold pressure as well as it describes CAC during fuel enrichment. It is therefore highly suitable for CAC estimation for control and diagnosis of turbocharged SI-engines.

ACKNOWLEDGMENTS

This work is funded by *Swedish Agency for Innovation Systems* and *Fiat-GM Powertrain Sweden*.

REFERENCES

[1] L. Guzzella, U. Wenger, and R. Martin. IC-Engine Downsizing and Pressure-Wave Supercharging for Fuel Economy. 2000. SAE Technical Paper No. 2000-01-1019.

[2] P. Degobert. *Automobiles and Pollution*. Society of Automotive Engineers, Inc., 1995.

[3] J.R. Mondt. *Cleaner Cars. The History and Technoloby of Emission Control Since the 1960s*. SAE International, 2000.

[4] John B. Heywood. *Internal Combustion Engine Fundamentals*. McGraw-Hill International Editions, 1988.

[5] Per B. Jensen, Mads B. Olsen, Jannik Poulsen, Elbert Hendricks, Michael Fons, and Christian Jepsen. A New Family of Nonlinear Observers for SI Engine Air/Fuel Ratio Control. In *Electronic Engine Controls*, SP-1236, pages 91–101, 1997. SAE Technical Paper No. 970615.

[6] J. David Powell, N. P. Fekete, and Chen-Fang Chang. Observer-Based Air-Fuel Ratio Control. *IEEE Control Systems*, 1998. 0272-1708/98.

[7] Seibum B. Choi and J. Karl Hedrick. An Observer-Based Controller Design Method for Improving Air/Fuel Characteristics of Spark Ignition Engines. *IEEE Transactions on Control Systems Technology*, 8(3):325–334, May 1998.

[8] Paul M. Frank. Fault diagnosis in dynamic systems using analytical and knowledge-based redundancy : A survey and some new results. *Automatica*, 26(3):459–474, May 1990.

[9] Mattias Nyberg and Lars Nielsen. Model Based Diagnosis for the Air Intake System of the SI-engine. 1997. SAE Technical Paper No. 970209.

[10] Lars Eriksson, Simon Frei, Christopher Onder, and Lino Guzzella. Control and Optimization of Turbo Charged Spark Ignited Engines. IFAC world congress, Barcelona, Spain, 2002.

[11] Charles Fayette Taylor. *The Internal-Combustion Engine in Theory and Practice*, volume 1. The M.I.T. Press, 2 edition, 1994.

[12] Elbert Hendricks, Alain Chevalier, Michael Jensen, and Spencer C. Sorenson. Modelling of the Intake Manifold Filling Dynamics. 1996. SAE Technical Paper No. 960037.

[13] Horst Bauer, Arne Cypra, Anton Beer, and Hans Bauer, editors. *Bosch Automotive Handbook*. Robert Bosch Gmbh, 4 edition, 1996.

[14] Uwe Kiencke and Lars Nielsen. *Automotive Control Systems. For Engine, Driveline, and Vehicle*. Springer-Verlag, 2000.

[15] Per Andersson and Lars Eriksson. Air-to-Cylinder Observer on a Turbocharged SI-Engine with Wastegate. In *Electronic Engine Controls*, SP-1585, pages 33–40. SAE 2001 World Congress, March 2001, Detroit, MI, USA, March 2001. SAE Technical Paper No. 2001-01-0262.

NOMENCLATURE

Symbol	Description
CAC	Cylinder air charge, the mass of air trapped in the cylinder(s) per cycle
EVC	Exhaust valve closing
IVC	Intake valve closing
p_{im}	Intake manifold pressure
p_{em}	Exhaust manifold pressure
T_{im}	Intake manifold temperature
T_{cyl}	Temperature of charge entering the cylinder
T_B	Temperature of air entering the intake manifold
γ_e	Ratio of exhaust gas specific heats, $\gamma_e = 1.33$
λ	Normalized air/fuel ratio
$\left(\frac{A}{F}\right)_s$	Stoichiometric air/fuel ratio
$C_{\eta_{vol}}$	Engine pumping parameter parameter in air-mass to cylinder model
C_1	Parameter governing the charge cooling effect by fuel evaporation
r_c	Compression ratio. For the engine used $r_c = 9.3$
V_c	Clearance volume
V_d	Total engine displacement volume
V_a	Volume of air in the cylinder
V_f	Volume of fuel in the cylinder
V_{af}	Volume of air and fuel in the cylinder
W_a	Measured air-mass flow
N	Engine Speed

A DERIVATION OF EXHAUST MANIFOLD PRESSURE DEPENDENT CAC MODEL

Exhaust manifold pressure dependent CAC models have been derived using energy balance in [11, pp. 510]. This model lacks parameters that can be tuned for a specific engine which makes it less suitable for air/fuel ratio control. Here another method is used which estimates the volume of inducted air V_a. It results in the following CAC model [10]:

$$\text{CAC} = \frac{p_{im} V_a}{R_{im} T_{im}} \tag{13}$$

Using the fact that the ideal gas law can be expressed as

$$\begin{aligned} V &= \frac{nRT}{p} = (n_1 + \ldots + n_n)\frac{RT}{p} \\ (V_1 + \ldots + V_n) &= (n_1 + \ldots + n_n)\frac{RT}{p} \\ V_i &= n_i \frac{RT}{p} \quad 1 \le i \le n \end{aligned}$$

This results in that the gases in the cylinder can be divided into volumes of air, fuel, and residual gases, which is illustrated to the right of Figure 6.

The volume of air V_a and evaporated fuel V_f is simply estimated by subtracting the volume that the residual gases occupies at intake valve closing (IVC) from the total volume.

$$\underbrace{V_a + V_f}_{\text{Volume of air and fuel}} = \underbrace{V_d + V_c}_{\text{Total cylinder volume}} - V_r$$

Residual gas volume at IVC is estimated by isentropic expansion of the residual gases from the conditions at exhaust valve closing (EVC). That is they expand from volume V_c which gases occupies at exhaust manifold pressure p_{em} to the volume V_r which they occupy at IVC and intake manifold pressure p_{im}:

$$V_r = \left(\frac{p_{em}}{p_{im}}\right)^{\frac{1}{\gamma_e}} V_c$$

Here the residual gas volume at EVC is assumed to be constant and equal to the clearance volume V_c. This is reasonable as the engine is not equipped with any cam phasing device and also by the fact that volumes change only slightly around TDC. The remaining volume, after the expansion of the residual gases to intake manifold pressure, is then compensated for the volume of the fuel vapor (all fuel is assumed to enter the cylinder as vapor). The volume of inducted air is then V_a:

$$\begin{aligned} V_{af} &= \left(\frac{r_c - \left(\frac{p_{em}}{p_{im}}\right)^{\frac{1}{\gamma_e}}}{r_c - 1}\right) V_d \\ V_a &= \frac{1}{1 + \frac{1}{\lambda\left(\frac{A}{F}\right)_s}} V_{af} \end{aligned}$$

In the Equations above the following identities have been used: $V_d + V_c = r_c V_c$ and $V_c = \frac{V_d}{r_c - 1}$.

To describe the pumping capabilities of the engine one tunable gain parameter $C_{\eta_{vol}}$ is introduced and inserted into Equation (13), and the final CAC model becomes:

$$\text{CAC} = \frac{p_{im}\, C_{\eta_{vol}} \overbrace{\frac{1}{1 + \frac{1}{\lambda\left(\frac{A}{F}\right)_s}} \left(\frac{r_c - \left(\frac{p_{em}}{p_{im}}\right)^{\frac{1}{\gamma_e}}}{r_c - 1}\right) V_d}^{V_a}}{R_{im} T_{im}} \tag{14}$$